Research Article | Vol. 29, No. 20 / 27 Sep 2021 / Optics Express 32691
Optics EXPRESS

Incoherent superposition of polychromatic light enables single-shot nondiffracting light-sheet microscopy

VAHID EBRAHIMI,[1,2] JIALEI TANG,[1,2] AND KYU YOUNG HAN[1,*]

[1]CREOL, The College of Optics and Photonics, University of Central Florida, Orlando, FL 32816, USA
[2]These authors contributed equally to this work
[*]kyhan@creol.ucf.edu

Abstract: We demonstrate single-shot nondiffracting light-sheet microscopy by the incoherent superposition of dispersed polychromatic light sources. We characterized our technique by generating a Bessel light-sheet with a supercontinuum light-source and a C-light-sheet using a diode laser, and demonstrated its applicability to fluorescence microscopy. We emphasize that our method is easily implementable and compatible with the requirements of high-resolution microscopy.

1. Introduction

Light-sheet fluorescence microscopy (LSFM) has been widely used for three-dimensional (3D) volumetric imaging of biological samples [1]. A light-sheet selectively illuminates a thin portion of the sample, and the emitted fluorescence is generally collected by an orthogonally placed objective, which enables optical sectioning [2,3], long-term live-cell imaging [4] and fast assessment of clinical samples [5]. Multiple methods have been used to generate light-sheets [6–12]. In particular, scanning a nondiffracting beam has shown promising results by improving axial resolution while maintaining a large field of view [13–19]. However, this requires complex components and causes increased photodamage due to the high peak intensity delivered to the sample compared to a light-sheet created by a cylindrical lens with a Gaussian beam [1,20]. To solve these issues, field synthesis has been reported [21], in which a focused line is scanned over the back focal plane (BFP) of the excitation objective lens rather than scanning at the imaging plane. This allows one to significantly simplify lattice light-sheet imaging systems [17] and reduces photobleaching in Bessel light-sheet microscopy. Additionally, a new class of light-sheets called a C-light-sheet was also demonstrated using field synthesis [22], which balanced high axial resolution with reduced side lobes. However, field synthesis still utilizes beam scanning at the BFP, thus requiring mechanical components.

Toward scanning-free nondiffracting light-sheet generation, we recently reported a new method based on the incoherent superposition of a one-dimensional (1D) coherent beam at the image plane [23]. The 1D coherent beam was generated by a light-emitting diode (LED) spatially filtered by a narrow slit, or a diode laser used with a custom fiber that converted a bundle to a linear array. The latter is a more attractive approach because of its higher light transmission efficiency; however, it needs a specially designed fiber and a phase scrambler to ensure incoherent superposition. Field synthesis achieved incoherent superposition temporally by scanning a focused line at the BFP within a single camera exposure, whereas our approach manipulated spatial coherence to achieve the same light-sheet as field synthesis using static components.

In this paper we exploit the temporal coherence of polychromatic light sources to create 1D coherent beams, which provides an efficient means for instantaneously generating a Bessel light-sheet or C-light-sheet. We characterize nondiffracting light-sheets from supercontinuum

#439338 https://doi.org/10.1364/OE.439338
Journal © 2021 Received 2 Aug 2021; revised 9 Sep 2021; accepted 10 Sep 2021; published 24 Sep 2021

Optics EXPRESS

and diode laser light sources, and apply the method to LSFM to image fluorescent beads and collagen samples.

2. Working principle

When a focused line is scanned over the BFP of an objective lens with an annular mask, it creates a Bessel light-sheet [21] or C-light-sheet [22] depending on the extent of the scanning range. We reason that if multiple focused lines of different wavelengths are simultaneously illuminated across the BFP, the resulting fields are incoherently superimposed at the imaging plane and produce nondiffracting light-sheets without scanning a focused line (Fig. 1). Note that technically they are *pseudo* nondiffracting or *pseudo* propagation-invariant beams but here we will call nondiffracting light-sheets for convenience.

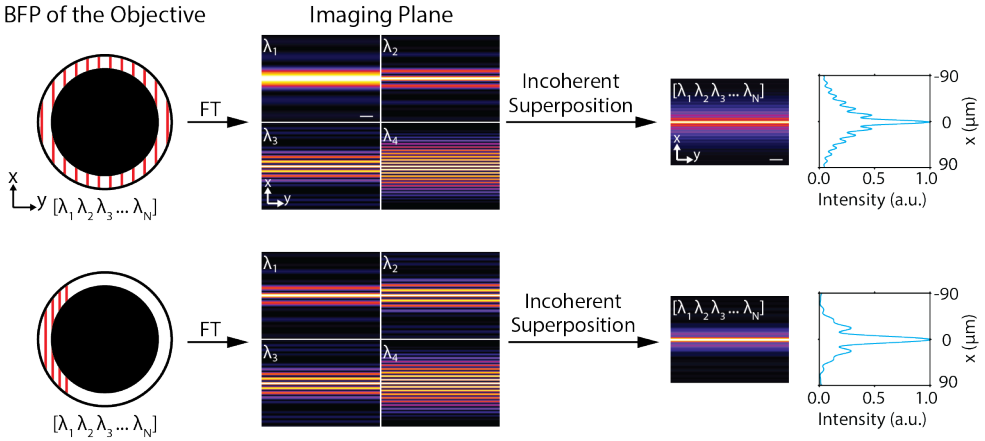

Fig. 1. Working principle of single-shot nondiffracting light-sheet generation by dispersed 1D coherent beams. Incoherent superposition of fields resulting from each different wavelength generates nondiffracting light-sheets such as Bessel light-sheet (top) or C-light-sheet (bottom). FT denotes Fourier transform. Scale bars, 50 μm.

We conceive that a combination of a diffraction grating and a cylindrical lens could create multiple focused lines (Fig. 2). Specifically, we call the focused line as a one-dimensional (1D) coherent beam which is coherent along the x-axis but incoherent along the y-axis at the BFP [23]. The grating separates light exiting from a polychromatic light source depending on the wavelength and the cylindrical lens focuses each wavelength of light as a line at the BFP of an objective. After interacting with a grating, the angular dispersion ($\Delta\theta$) of a polychromatic beam with a central wavelength λ_0 and bandwidth $\Delta\lambda$ can be described as:

$$\Delta\theta = \tan\theta \frac{\Delta\lambda}{\lambda_0}, \tag{1}$$

$$\theta = \sin^{-1}\left(\frac{\lambda_0}{D_g}\right), \tag{2}$$

where θ is the angle of the first order diffracted beam when the incident beam is normal to the grating surface and D_g is the space of the grating. The beam is dispersed at the BFP along the y-axis, and if the angular dispersion is small, the amount of geometric dispersion (d_y) can be

Optics EXPRESS

approximated as:

$$d_y = f_{CL}\Delta\theta, \tag{3}$$

where f_{CL} is the focal length of the cylindrical lens. It is possible to make this linear relationship valid over a wide range of angular dispersion if an achromatic f-theta lens is used. A similar configuration has been used in two-photon excitation microscopy for temporal focusing [24,25], although for a different purpose.

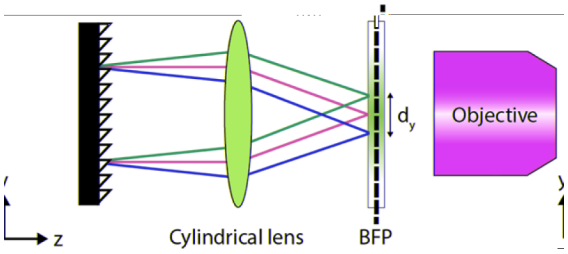

Fig. 2. Experimental scheme for creating 1D coherent beams using polychromatic light. A reflective diffraction grating followed by a cylindrical lens disperses light and focuses them at an annulus placed at the back focal plane of an objective lens.

3. Methods

3.1. Experimental setup

We used a custom-made light-sheet microscope as shown in Fig. 3. A supercontinuum light source (WhiteLase, NKT Photonics) or a diode laser (06-MLD, Cobolt) was used to generate the nondiffracting light-sheet. The former was expanded by two lenses L1 and L2 ($f_1 = 25.4$ mm, $f_2 = 400$ mm), and the latter was spatially filtered by a single-mode fiber (S405-XP) and collimated by a lens L3 ($f_3 = 75$mm). Note that high spatial coherence is a prerequisite of an input beam to generate nondiffracting light-sheets [23,26]. The beam was sent to a reflective diffraction grating ($D_g = 833$ nm, GR25-1205) and a cylindrical lens CL ($f_{CL} = 150$ mm or 250 mm). An annular mask (R1CA2000) with an outer radius (b) of 1 mm and an inner radius (a) of 0.85 mm was placed at the conjugated BFP, which was relayed by a 1:1 imaging system ($f_4 = f_5 = 60$ mm) to the BFP of the excitation objective ($f_{obj} = 18$ mm, LMPLFLN 10×/0.28, Olympus). The emitted fluorescence signal was captured by a detection objective (UPLFLN 4×/0.13, UPLFLN 10×/0.3 or MPLFLN 50×/0.8; Olympus), filtered by a bandpass filter (ET700/75, Chroma) and imaged onto a camera (GS3-U3-51S5M-C, FLIR) by a lens L8 ($f_8 = 150$ mm). We measured the spectrum of the diode laser with a spectrometer (HR4000, Ocean Optics) and fit the results to a Gaussian profile to calculate the linewidth of the light-source.

To obtain 3D image stacks, the sample was mounted on a motorized stage (PT1-Z8) and moved along the x-axis, i.e., along the optical axis of the detection objective. For beam profile measurements, the generated light-sheet was imaged by a pair of lenses ($f_6 = 40$ mm and $f_7 = 100$ mm) on a second camera (BFS-U3-200S6M-C, FLIR) mounted on a motorized stage [23]. In the case of the supercontinuum light source, the output beam was filtered by a bandpass filter (FF01-635/18-25 or FF01-637/7-25, Semrock), a cylindrical lens with $f_{CL} = 150$ mm was used, and an achromatic lens ($f_{obj} = 40$ mm) was used as an objective. Optics and optomechanical components were purchased from Thorlabs unless specified otherwise.

3.2. Sample preparation

1 μm diameter fluorescent beads (F8816, ThermoFisher) were mixed with a hydrogel solution which was made of 7.5% acrylamide:bisacrylamide (29 : 1) (National Diagnostics), 0.2% (v/v)

Optics EXPRESS

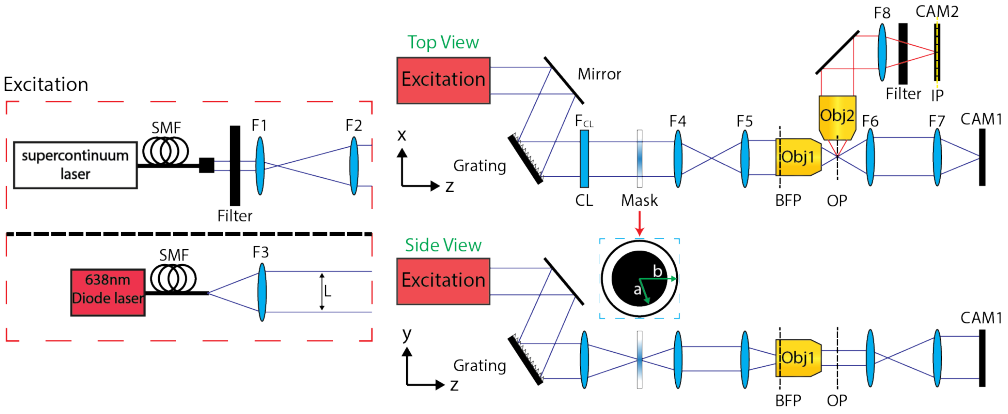

Fig. 3. Experimental setup of the single-shot nondiffracting light-sheet microscope. A diode laser (top) or a supercontinuum light source (bottom) was used as an excitation source. CAM1-2, cameras; CL, cylindrical lens; L1-8, lenses; SMF, single-mode fiber. a and b denote inner and outer radius, respectively.

tetramethylethylenediamine (TEMED), and 0.02% (w/v) ammonium persulfate in 0.75× TAE buffer (tris-acetate-EDTA) [27]. 100 µL of the mixture was injected into a flow chamber (155409, ThermoFisher) and incubated for 10 min. The polymerized hydrogel was mounted on a glass slide for imaging.

For 3D collagen samples, rat-tail collagen (A1048301, ThermoFisher) at a concentration of 3 mg/mL was labeled with Atto-647 NHS ester (07376, Sigma-Aldrich) [28]. 5% of the labeled collagen was mixed with a 95% of unlabeled collagen. 50 µL of the collagen solution (1.5 mg/mL) was mixed with 10 µL of 10× PBS, 0.3 µL of 1N sodium hydroxide, and 39.7 µL of distilled water. All the solutions were pre-chilled to prevent any immature polymerization. 50 µL of the final solution was injected into a flow chamber and incubated at room temperature for one hour. The degree of polymerization of the sample was checked with a phase contrast microscope every 15 minutes.

4. Results

4.1. Single-shot Bessel light-sheet generation by supercontinuum light

We used a supercontinuum light source to prove our method of nondiffracting light-sheet generation. To ensure that the 1D coherent beams fully covered the annulus, an 18 nm bandwidth filter centered at $\lambda_0 \sim 635$ nm was used, which provided ~5.0 mm of geometric dispersion, d_y. We recorded intensity profiles of three different cases using supercontinuum light (Fig. 4): (i) a Bessel beam, (ii) Gaussian light-sheet, and (iii) Bessel light-sheet. For the Bessel beam, the grating and cylindrical lens were omitted, and for the Gaussian light-sheet the annular mask was removed. Figure 4(c) shows that our approach was able to produce a Bessel light-sheet without scanning a focused line over the BFP. Please note that the Bessel light-sheet is conventionally generated by scanning a Bessel beam, so the side lobes are superposed (Fig. 4(d)). The propagation length of the Bessel light-sheet was ~5.5 times longer (7.34 mm) than the Gaussian light-sheet (1.34 mm) while its thickness measured at the full width at half maximum (FWHM) of the main lobe

Optics EXPRESS

was ~0.7 smaller (8.8 μm) than that of the Gaussian light-sheet (11.8 μm). A narrow bandwidth ($\Delta\lambda = 7$ nm) yielded a similar result.

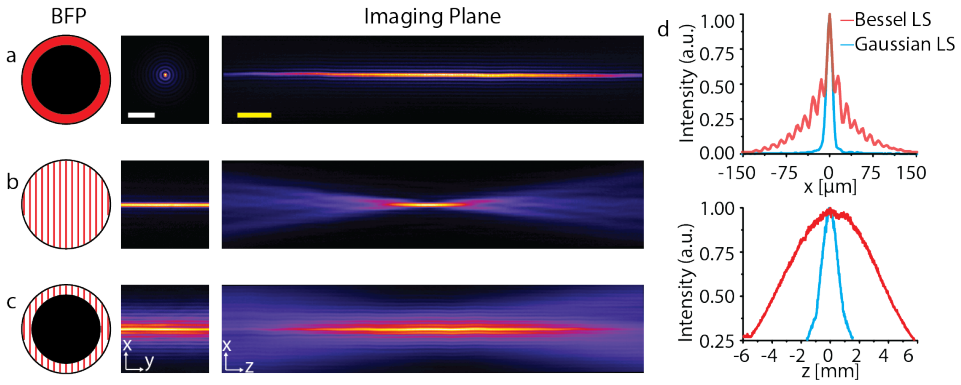

Fig. 4. Light-sheet intensity profiles generated by a supercontinuum light source. (a) Bessel beam. (b) Gaussian light-sheet. (c) Bessel light-sheet. (d) Line profiles of Gaussian (blue) and Bessel (red) light-sheets along the x-axis (top) and z-axis (bottom). Scale bars, 100 μm (white) and 1 mm (yellow).

4.2. *Single-shot C-light-sheet generation by a diode laser*

A supercontinuum is unlikely to be an ideal light source in LSFM for long-term observation, because pulsed excitation can induce photodamage [1,20,29]. A more desirable light source may be a continuous wave (CW) diode laser. However, these usually have a narrow spectral bandwidth in the range of 1−3 nm, which prevents 1D coherent beams from covering the entire annulus in accordance with Eqs. (1)–(3). Although a Bessel light-sheet cannot be generated in this case, a C-light-sheet [22] can be created by illuminating a portion of the annulus (Fig. 5(a)).

We experimentally demonstrated our concept using a diode laser emitting a wavelength of 638 nm with $\Delta\lambda = 1.4$ nm (Fig. 5(b)) by measuring the intensity profiles for a Gaussian light-sheet and C-light-sheet in a similar way to those using the supercontinuum source. We adjusted the position of the 1D coherent beams such that they covered a 0.43-0.85 mm range of the BFP when a cylindrical lens with $f_{CL} = 250$ mm was used. Our results showed that the narrow bandwidth of the diode laser was sufficient to produce a single-shot C-light-sheet (Fig. 5(a)). The propagation length of the C-light-sheet was $\Delta z = 1.16$ mm, which was ~2-times longer than the Gaussian light-sheet ($\Delta z = 0.64$ mm) for the same light-sheet thickness ($\Delta x = 5.9$ μm), as shown in Figs. 5(c) and 5(d).

4.3. *Fluorescence imaging with single-shot C-light-sheet microscopy*

We imaged 1 μm fluorescent beads embedded in a 3D hydrogel using our light-sheet microscope with the diode laser. The longer propagation length of a C-light-sheet allowed us to have a 1.8-fold larger field-of-view (FOV) compared to a Gaussian light-sheet (Figs. 6(a) and 6(b)). To quantify the size of FOV, we averaged the pixel values in the y direction, smoothed the curve and fitted it with a Gaussian function. We were also able to obtain high resolution 3D images by translating the hydrogel over a 30 μm depth using a 50×/0.8 detection objective (Figs. 6(c) and 6(d)). Contrast reduction due to side lobes of a C-light-sheet was negligible because the axial detection point spread function was smaller than the light-sheet thickness.

Optics EXPRESS

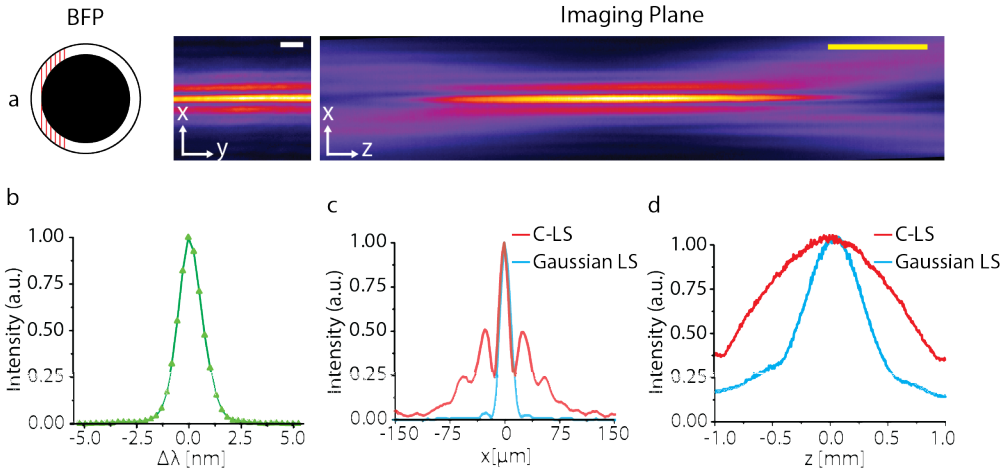

Fig. 5. Single-shot C-light-sheet generation using a diode laser. The beam covers a range of 0.43-0.85mm at the BFP. (a) Intensity profiles of single-shot C-light-sheet. (b) Spectrum of the diode laser. Line profiles in the *x*-axis (c) and *z*-axis (d) for the Gaussian light-sheet (blue) and C-light-sheet (red). Scale bars, 25 μm (white) and 400 μm (yellow).

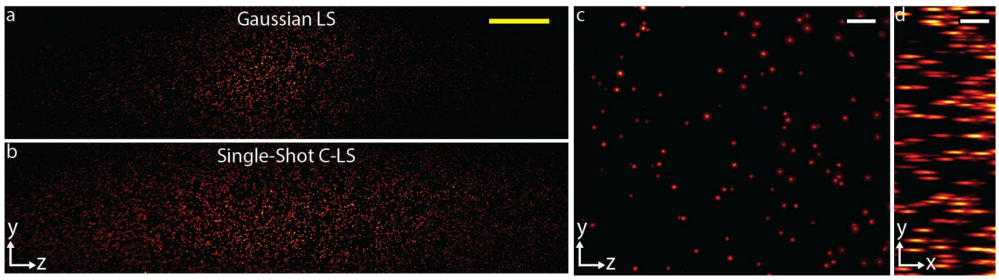

Fig. 6. Fluorescence images of 1 μm beads in 3D hydrogels measured by Gaussian light-sheet (a) and single-shot C-light-sheet microscopy (b-d). The detection objectives were 4×/0.13 for (a, b) and 50×/0.8 for (c, d). All images were maximum intensity projected. Scale bars, 10 μm (white) and 200 μm (yellow).

Optics EXPRESS

Lastly, we imaged 3D collagen samples with our microscope. A comparison of the same imaging areas taken using a Gaussian light-sheet and a C-light-sheet clearly emphasize the increased FOV of the C-light-sheet (Fig. 7). The images show the diffraction-limited performance and minimal out-of-focus background, as expected.

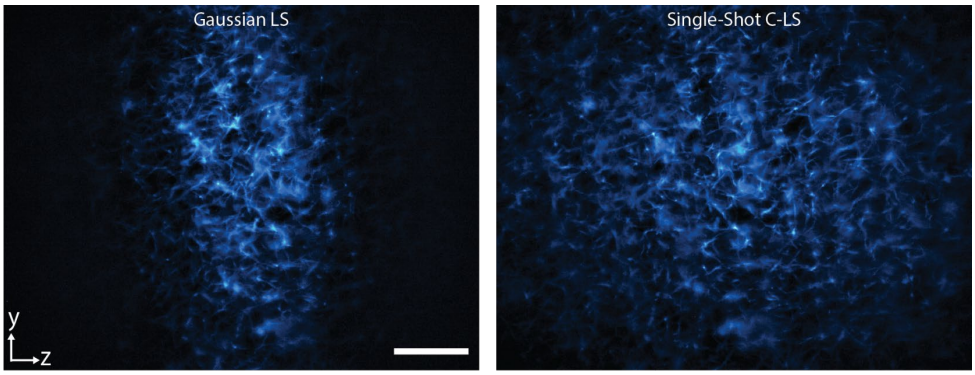

Fig. 7. Rat-tail collagen labeled with Atto647N imaged by a Gaussian light-sheet (left) and a single-shot C-light-sheet (right). The detection objective lens was 20×/0.5. Scale bar, 150 μm.

5. Discussion

We demonstrated single-shot nondiffracting light-sheet microscopy using spatially coherent polychromatic light. In contrast with other approaches [14,16,17,21,22], our method of illuminating an annular mask using dispersed light makes the use of a galvo scanner and/or SLM unnecessary in the illumination part. In fluorescence microscopy, the inherent bandwidth of polychromatic light sources has not been extensively exploited except for multicolor imaging using a white light laser [30]; although, dispersed illumination has been used for other imaging modalities [31]. Here, we utilized the temporal coherence of light to achieve the incoherent superposition of multiple light-sheets. In principle, this may be applicable to other fluorescence imaging techniques [32]. If the annular mask is omitted, a single-shot multidirectional Gaussian light-sheet will be generated, which can reduce shadowing effects [33].

One may notice that the illumination FOV along the y-axis (FOV_y) appears smaller than that along the z-axis. This is attributed to the fact that FOV_y is governed by the magnification and the diameter of collimated input beam (L). If L and d_y are kept constant, FOV_y is proportional to $\Delta\lambda$ based on Eqn. (1). However, this is often not an issue because the FOV is typically limited by the propagation length of light-sheets, especially for high resolution microscopy.

Unlike our previous technique [23] which generated 1D coherent beams via controlling spatial coherence, there is no need for a custom fiber nor fiber shaker. As many diode lasers used in fluorescence microscopy have bandwidths similar to that of our tested laser, our approach is readily applicable to multicolor fluorescence light-sheet imaging. Other light sources such as superluminescent diodes [34] can be also utilized in our technique. Further studies comparing other single-shot *pseudo* nondiffracting light-sheets [35–39] will give us insight on the properties of these light-sheets, especially comparisons with Gaussian light-sheets [40,41]. We expect our method can simplify non-diffracting light-sheet microscopes.

Funding. National Institutes of Health (R35GM138039); University of Central Florida (65019A04).

Optics EXPRESS

Acknowledgments. We thank to NKT Photonics for loaning the supercontinuum laser, David J. Hagan for letting us to use the spectrometer, and Benjamin Croop for critically reading our manuscript.

Disclosures. The authors declare no conflicts of interest.

Data Availability. Data underlying the results presented in this paper are not publicly available at this time but may be obtained from the authors upon reasonable request.

References

1. R. M. Power and J. Huisken, "A guide to light-sheet fluorescence microscopy for multiscale imaging," Nat. Methods **14**(4), 360–373 (2017).
2. O. E. Olarte, J. Andilla, E. J. Gualda, and P. Loza-Alvarez, "Light-sheet microscopy: a tutorial," Adv. Opt. Photonics **10**(1), 111–179 (2018).
3. J. M. Girkin and M. T. Carvalho, "The light-sheet microscopy revolution," J. Opt. **20**(5), 053002 (2018).
4. L. A. Royer, W. C. Lemon, R. K. Chhetri, Y. Wan, M. Coleman, E. W. Myers, and P. J. Keller, "Adaptive light-sheet microscopy for long-term, high-resolution imaging in living organisms," Nat. Biotechnol. **34**(12), 1267–1278 (2016).
5. A. K. Glaser, N. P. Reder, Y. Chen, E. F. McCarty, C. Yin, L. Wei, Y. Wang, L. D. True, and J. T. C. Liu, "Light-sheet microscopy for slide-free non-destructive pathology of large clinical specimens," Nat. Biomed. Eng. **1**, 0084 (2017).
6. J. Huisken, J. Swoger, F. Del Bene, J. Wittbrodt, and E. H. K. Stelzer, "Optical sectioning deep inside live embryos by selective plane illumination microscopy," Science **305**(5686), 1007–1009 (2004).
7. P. J. Keller, A. D. Schmidt, J. Wittbrodt, and E. H. K. Stelzer, "Reconstruction of zebrafish early embryonic development by scanned light sheet microscopy," Science **322**(5904), 1065–1069 (2008).
8. K. M. Dean, P. Roudot, E. S. Welf, G. Danuser, and R. Fiolka, "Deconvolution-free subcellular imaging with axially swept light sheet microscopy," Biophys. J. **108**(12), 2807–2815 (2015).
9. L. Gao, "Extend the field of view of selective plan illumination microscopy by tiling the excitation light sheet," Opt. Express **23**(5), 6102–6111 (2015).
10. C. Garbellotto and J. M. Taylor, "Multi-purpose SLM-light-sheet microscope," Biomed. Opt. Express **9**(11), 5419–5436 (2018).
11. R. McGorty, D. Xie, and B. Huang, "High-NA open-top selective-plane illumination microscopy for biological imaging," Opt. Express **25**(15), 17798–17810 (2017).
12. A. K. Gustavsson, P. N. Petrov, and W. E. Moerner, "Light sheet approaches for improved precision in 3D localization-based super-resolution imaging in mammalian cells [Invited]," Opt. Express **26**(10), 13122–13147 (2018).
13. F. O. Fahrbach, P. Simon, and A. Rohrbach, "Microscopy with self-reconstructing beams," Nature Photon **4**(11), 780–785 (2010).
14. T. A. Planchon, L. Gao, D. E. Milkie, M. W. Davidson, J. A. Galbraith, C. G. Galbraith, and E. Betzig, "Rapid three-dimensional isotropic imaging of living cells using Bessel beam plane illumination," Nat. Methods **8**(5), 417–423 (2011).
15. F. O. Fahrbach, V. Gurchenkov, K. Alessandri, P. Nassoy, and A. Rohrbach, "Self-reconstructing sectioned Bessel beams offer submicron optical sectioning for large fields of view in light-sheet microscopy," Opt. Express **21**(9), 11425–11440 (2013).
16. T. Vettenburg, H. I. C. Dalgarno, J. Nylk, C. Coll-Llado, D. E. K. Ferrier, T. Cizmar, F. J. Gunn-Moore, and K. Dholakia, "Light-sheet microscopy using an Airy beam," Nat. Methods **11**(5), 541–544 (2014).
17. B.-C. Chen, W. R. Legant, K. Wang, L. Shao, D. E. Milkie, M. W. Davidson, C. Janetopoulos, X. S. Wu, III J. A. Hammer, Z. Liu, B. P. English, Y. Mimori-Kiyosue, D. P. Romero, A. T. Ritter, J. Lippincott-Schwartz, L. Fritz-Laylin, R. D. Mullins, D. M. Mitchell, J. N. Bembenek, A.-C. Reymann, R. Boehme, S. W. Grill, J. T. Wang, G. Seydoux, U. S. Tulu, D. P. Kiehart, and E. Betzig, "Lattice light-sheet microscopy: Imaging molecules to embryos at high spatiotemporal resolution," Science **346**, 439 (2014).
18. G. Di Domenico, G. Ruocco, C. Colosi, E. Delre, and G. Antonacci, "Cancellation of Bessel beam side lobes for high-contrast light sheet microscopy," Sci. Rep. **8**(1), 17178 (2018).
19. S. Ryu, B. Seong, C.-W. Lee, M. Y. Ahn, W. T. Kim, K.-M. Choe, and C. Joo, "Light sheet fluorescence microscopy using axi-symmetric binary phase filters," Biomed. Opt. Express **11**(7), 3936–3951 (2020).
20. J. Tang, J. Ren, and K. Y. Han, "Fluorescence imaging with tailored light," Nanophotonics **8**(12), 2111–2128 (2019).
21. B.-J. Chang, M. Kittisopikul, K. M. Dean, P. Roudot, E. S. Welf, and R. Fiolka, "Universal light-sheet generation with field synthesis," Nat. Methods **16**(3), 235–238 (2019).
22. B.-J. Chang and R. Fiolka, "Light-sheet engineering using the Field Synthesis theorem," J. Phys. Photonics **2**(1), 014001 (2020).
23. J. Tang and K. Y. Han, "Instantaneous non-diffracting light-sheet generation by controlling spatial coherence," Opt. Comm. **474**, 126154 (2020).
24. E. Tal, D. Oron, and Y. Silberberg, "Improved depth resolution in video-rate line-scanning multiphoton microscopy using temporal focusing," Opt. Lett. **30**(13), 1686–1688 (2005).
25. G. H. Zhu, J. van Howe, M. Durst, W. Zipfel, and C. Xu, "Simultaneous spatial and temporal focusing of femtosecond pulses," Opt. Express **13**(6), 2153–2159 (2005).

Optics EXPRESS

26. P. Fischer, C. T. A. Brown, J. E. Morris, C. López-Mariscal, E. M. Wright, W. Sibbett, and K. Dholakia, "White light propagation invariant beams," Opt. Express **13**(17), 6657–6666 (2005).
27. J. Tang and K. Y. Han, "Extended field-of-view single-molecule imaging by highly inclined swept illumination," Optica **5**(9), 1063–1069 (2018).
28. A. D. Doyle, "Generation of 3D Collagen Gels with Controlled Diverse Architectures," Curr. Protoc. Cell Biol. **72**(1), 10–20 (2016).
29. L. Gao, L. Shao, C. D. Higgins, J. S. Poulton, M. Peifer, M. W. Davidson, X. Wu, B. Goldstein, and E. Betzig, "Noninvasive imaging beyond the diffraction limit of 3D dynamics in thickly fluorescent specimens," Cell **151**(6), 1370–1385 (2012).
30. J. B. Pawley, *Handbook of biological confocal microscopy* (Plenum, 2006).
31. G. J. Tearney, R. H. Webb, and B. E. Bouma, "Spectrally encoded confocal microscopy," Opt. Lett. **23**(15), 1152–1154 (1998).
32. B. Croop, J. Tang, and K. Y. Han, "Single-shot, shadowless total internal reflection fluorescencemicroscopy via annular fiber bundle," Opt. Lett. **45**(23), 6470–6473 (2020).
33. J. Huisken and D. Y. R. Stainier, "Even fluorescence excitation by multidirectional selective plane illumination microscopy (mSPIM)," Opt. Lett. **32**(17), 2608–2610 (2007).
34. G. A. Alphonse, D. B. Gilbert, M. G. Harvey, and M. Ettenberg, "High-Power Superluminescent Diodes," IEEE J. Quantum Electron. **24**(12), 2454–2457 (1988).
35. Z. Yang, M. Prokopas, J. Nylk, C. Coll-Lladó, F. J. Gunn-Moore, D. E. K. Ferrier, T. Vettenburg, and K. Dholakia, "A compact Airy beam light sheet microscope with a tilted cylindrical lens," Biomed. Opt. Express **5**(10), 3434–3442 (2014).
36. T. Zhao, S. C. Lau, Y. Wang, Y. M. Su, H. Wang, A. F. Cheng, K. Herrup, N. Y. Ip, S. W. Du, and M. M. T. Loy, "Multicolor 4D fluorescence microscopy using ultrathin bessel light sheets," Sci. Rep. **6**(1), 26159 (2016).
37. T. C. Fadero, T. M. Gerbich, K. Rana, A. Suzuki, M. DiSalvo, K. N. Schaefer, J. K. Heppert, T. C. Boothby, B. Goldstein, M. Peifer, N. L. Allbritton, A. S. Gladfelter, A. S. Maddox, and P. S. Maddox, "LITE microscopy: Tilted light-sheet excitation of model organisms offers high resolution and low photobleaching," J. Cell. Biol. **217**(5), 1869–1882 (2018).
38. M. Yessenov, B. Bhaduri, H. E. Kondakci, M. Meem, R. Menon, and A. F. Abouraddy, "Non-diffracting broadband incoherent space-time fields," Optica **6**(5), 598–607 (2019).
39. S. Du, T. Zhao, and L. Zhao, "Light sheets with extended length," Opt. Comm. **450**, 166–171 (2019).
40. E. Remacha, L. Friedrich, J. Vermot, and F. O. Fahrbach, "How to define and optimize axial resolution in light-sheet microscopy: a simulation-based approach," Biomed. Opt. Express **11**(1), 8–26 (2020).
41. B.-J. Chang, K. M. Dean, and R. Fiolka, "Systematic and quantitative comparison of lattice and Gaussian light-sheets," Opt. Express **28**(18), 27052–27077 (2020).